

This is a repository copy of *Enzymatic synthesis of biobased polyesters utilizing aromatic diols as the rigid component*.

White Rose Research Online URL for this paper:

<https://eprints.whiterose.ac.uk/159725/>

Version: Published Version

Article:

Pellis, Alessandro, Weinberger, Simone, Gigli, Matteo et al. (2 more authors) (2020)
Enzymatic synthesis of biobased polyesters utilizing aromatic diols as the rigid component.
European Polymer Journal. 109680. pp. 1-8. ISSN 0014-3057

<https://doi.org/10.1016/j.eurpolymj.2020.109680>

Reuse

This article is distributed under the terms of the Creative Commons Attribution (CC BY) licence. This licence allows you to distribute, remix, tweak, and build upon the work, even commercially, as long as you credit the authors for the original work. More information and the full terms of the licence here:

<https://creativecommons.org/licenses/>

Takedown

If you consider content in White Rose Research Online to be in breach of UK law, please notify us by emailing eprints@whiterose.ac.uk including the URL of the record and the reason for the withdrawal request.



Enzymatic synthesis of biobased polyesters utilizing aromatic diols as the rigid component

Alessandro Pellis^{a,b,*}, Simone Weinberger^b, Matteo Gigli^c, Georg M. Guebitz^{b,d}, Thomas J. Farmer^a

^a University of York, Department of Chemistry, Green Chemistry Centre of Excellence, Heslington, York YO10 5DD, UK

^b University of Natural Resources and Life Sciences Vienna, Department of Agrobiotechnology, Institute of Environmental Biotechnology, 3430 Tulln an der Donau, Austria

^c University of Venice Ca' Foscari, Department of Molecular Sciences and Nanosystems, Via Torino 155, 30172 Venezia Mestre, Italy

^d Austrian Centre of Industrial Biotechnology, 3430 Tulln an der Donau, Austria

ARTICLE INFO

Keywords:

Biocatalyzed synthesis

Aromatic diols

Polycondensation

Pyridine derivatives

Bio-based polyesters

ABSTRACT

In the present work, the biocatalyzed synthesis of a series of aromatic-aliphatic polyesters based on the aliphatic diesters dimethyl succinate, dimethyl adipate and dimethyl sebacate and the aromatic diols 2,5-bis(hydroxymethyl)furan, 3,4-bis(hydroxymethyl)furan and 2,6-pyridinedimethanol were investigated. A similar series of polyesters based on the petroleum-based 1,3-benzenedimethanol, 1,4-benzenedimethanol and 1,4-benzenediethanol were also synthesized for comparison. Data show that the enzymatic syntheses were successful starting from all diols, with the obtained polymers having isolated yields between 67 and over 90%, number average molecular weights between 3000 Da and 5000 Da and degree of polymerization (DP) of 6–18 (based on the used aliphatic diesters and aromatic diols) when polymerized in diphenyl ether as solvent. Only using 3,4-bis(hydroxymethyl)furan as the diol led to shorter oligomers with isolated yields around 50% and DPs of 3–5. DSC and TGA thermal analyses show clear correlation between polymer crystallinity and aliphatic carbon chain length of the diester.

1. Introduction

With the society's increasing awareness and concern towards the use and disposal of single use plastics, governments and private enterprises are combining efforts to reduce plastic-derived pollution [1]. Work toward increasing plastic recyclability, reduction of pollution and synthesizing alternative bio-materials from renewable sources is aimed to reduce our dependence from non-renewable petroleum-based raw materials. Hence, the use of resources like plastic garbage as feedstock [2] would allow the plastic industry to close the carbon cycle [3]. Studies on the replacement of terephthalic acid (TA) with bio-based TA [4] or its furan-based counterpart, i.e. 2,5-furandicarboxylic acid, indicated the possibility to synthesize furan diacid-based polyesters and co-polyesters using both traditional chemocatalysis [5,6] or enzymatic synthesis [7,8]. Most previous studies indeed focused on synthesis of poly(ethylene-2,5-furandicarboxylate) (PEF) that is aimed to substitute poly(ethylene terephthalate) (PET) in the production of water and soft drinks bottles. Furan-based alternative polyesters such as poly(1,4-butylene 2,5-furandicarboxylate) [9], poly(1,4-butylene 2,5-

thiophenedicarboxylate) [10–12] and various copolymers containing a wide range of aliphatic diols and diesters [13] were also investigated and showed interesting barrier properties that could lead to their use as film packaging.

All these materials, despite the advantage of being bio-based, are enzymatically better degradable than the petrol-based PET and it is therefore easier to recycle them using biotechnological methods. In fact, while PET can be only partially degraded, with reported weight losses usually between 5% and 20% [14,15], PEF can be completely degraded into its constituent monomers and soluble oligomers in three days [16].

More recently, lignin-derived diesters simply called pyridinedicarboxylic acids were also suggested for the substitution of the terephthalic unit. These monomers might offer increased rigidity if incorporated into a polymer, yet retaining a potentially interesting functionality which may affect the stacking/crystallization behaviour of the polycondensation product [17].

Despite the fact that several studies tried to substitute TA with various aromatic diesters, only few attempts were made towards the

* Corresponding author at: University of Natural Resources and Life Sciences Vienna, Department of Agrobiotechnology, Institute of Environmental Biotechnology, Konrad Lorenz Strasse 20, 3430 Tulln an der Donau, Austria.

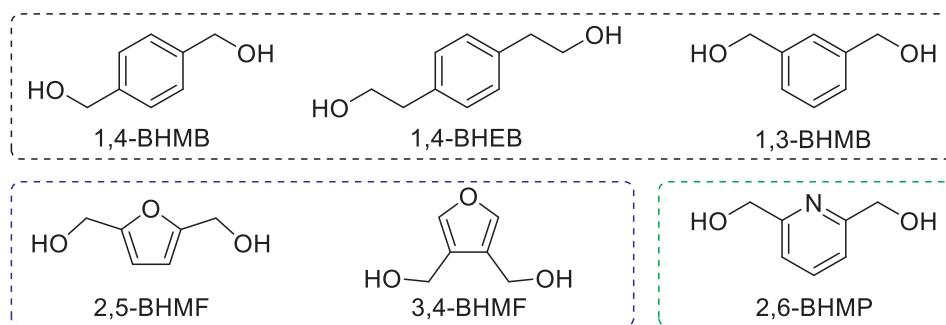
E-mail address: alessandro.pellis@boku.ac.at (A. Pellis).

<https://doi.org/10.1016/j.eurpolymj.2020.109680>

Received 25 February 2020; Received in revised form 3 April 2020; Accepted 6 April 2020

Available online 07 April 2020

0014-3057/ © 2020 The Authors. Published by Elsevier Ltd. This is an open access article under the CC BY license (<http://creativecommons.org/licenses/by/4.0/>).



Scheme 1. Monomers used for the enzymatic polycondensation reactions. Benzene-based (top, black frame), furan-based (bottom left, blue frame) and pyridine-based (bottom right, green frame) monomers with the related polymers.

utilization of aromatic diols for giving rigidity to the polyester chain. A first attempt using 2,5-bis(hydroxymethyl)furan (2,5-BHMF) as the diol was made by Loos and co-workers who synthesized a series of aliphatic-aromatic polyesters using a three-stage method (obtained $M_n \approx 2000$ Da) [16] and further investigated copolymers containing both 2,5-BHMF and diethyl-2,5-furandicarboxylate that achieved polymers having higher molecular weights [18,19]. Other isosorbide-like diols were also used to give rigidity to the polymer chain in various extends (despite it leads to a decrease in crystallinity), with all relative works on the topic employ traditional metal compounds as the catalysts [20,21] (see Scheme 1).

The focus of this paper is directed at the investigation of the biocatalyzed synthesis of furan- and pyridine-derived aromatic diols polyesters, along with characterization of their thermal properties. A series of aromatic-aliphatic polyesters based on benzene-derived diols are also synthesized for comparison with the bio-based monomers.

2. Results and discussion

The synthesis of the aromatic diols-based polyesters was conducted in diphenyl ether (DPE) as reaction solvent. This synthesis method was selected because some of the dimethanol diols used in the study have melting temperatures (see Supplementary Table 1) above the enzyme's deactivation temperature. Therefore, solventless synthesis protocols reported for other aliphatic and aromatic monomers was deemed inappropriate for this study. The DPE-based synthesis employed immobilized *Candida antarctica* lipase B (iCaLB) as the catalyst and was successful for all selected aromatic diols.

2.1. Synthesis of furan diols-based polyesters

We initiated the study on two furan-containing bio-derivable diols, namely 2,5-bis(hydroxymethyl)furan (2,5-BHMF) and 3,4-bis(hydroxymethyl)furan (3,4-BHMF). The enzymatic synthesis of 2,5-BHMF-based polyesters using various aliphatic diols was recently reported by Loos and co-workers [18], while the use of 3,4-BHMF as the diol, at best of our knowledge, has never been reported before for enzymatic polycondensations.

In Table 1, the polymerization products obtained using 2,5-BHMF as the diol in this work (t.w.) are compared with the data previously reported in the literature [18]. The obtained results are in line in terms of thermal properties and number average molecular weight (M_n) from those previously published, while differences in weight average molecular weight (M_w) and dispersity (\bar{D}), with all polymers synthesized in the present work having higher M_w and \bar{D} values. These differences are likely the result of alternative synthesis and purification protocols.

After these first polycondensation reactions we performed the same synthesis substituting the 2,5-BHMF with 3,4-BHMF to elucidate if such furan-derived polyols have similar or different reactivities when they undergo a lipase-catalyzed transesterification. As shown by the data plotted in Fig. 1A, using 3,4-BHMF as the diol leads to lower recovered

Table 1

Comparison of the polymers obtained using 2,5-BHMF and the aliphatic succinic (C_4 , pF₂₅S), adipic (C_6 , pF₂₅A) and sebacic (C_{10} , pF₂₅Se) ester derivatives.

Polymer	T _g ^a [°C]	T _c ^a [°C]	T _m ^a [°C]	M _n ^b [Da]	M _w ^b [Da]	\bar{D} ^b	Yield ^c [%]	Ref.
pF ₂₅ S	4	–	–	2100	2700	1.29	60	[18]
	10	–	–	3100	8000	2.66	77	t.w.
pF ₂₅ A	–19	–	–	2200	3400	1.55	64	[18]
	–15	–	–	2800	25,400	11.98	69	t.w.
pF ₂₅ Se	–29	28	69/79	2200	3600	1.64	62	[18]
	–22	41	81	3000	20,400	7.77	66	t.w.

t.w. = this work.

^a T_g = glass transition temperature (2nd heating), T_c = crystallization temperature (1st cooling), T_m = melting temperature (2nd heating). Calculated via DSC.

^b M_n = number average molecular weight, M_w = weight average molecular weight, \bar{D} = dispersity. Calculated via CHCl₃ GPC.

^c Isolated yield after ice-cold MeOH precipitation and three washing steps. Used formula: yield [%] = [recovered amount of polymer (mg)] * 100/[theoretical 100% conversion (mg)].

yields (49% vs 77% for DMS, 49% vs 69% for DMA and 56% vs 66% for DMSe). Following the decreasing trends observed for the isolated yields, also the polymer's M_n s dropped by around 2/3 (from ~3000 Da to less than 1000 Da) in all cases (Fig. 1B).

The 3,4-BHMF-based polymers thermal properties were also assessed via DSC and TGA analysis (see Supplementary Table 2 for the DSC and Supplementary Table 3 for the TGA complete set of data). Thermograms of the DMS-based polymer resulted in a totally amorphous polymer having a T_g of –1 °C (Fig. 2A, blue line) while those containing DMA (Fig. 2A, red line) and DMSe (Fig. 2A, green line) T_g's of –28 °C and –39 °C as well as a T_m of 189 °C and 170 °C respectively. This increase in crystallinity of the obtained polymers, similarly observed for the 2,5-BHMF polymers, is likely due to the fact that the crystallization ability of the polyesters is boosted by the enhancement of the number of methylene units in the polyester main chain. These results are in line with previous reports that have shown a similar behaviour of furan diols [18] and isohexide-based polyesters [22]. TGA analysis shows that the 3,4-BHMF polymers have T_{d50%} between 358 and 385 °C (Fig. 2B), while polymers based on the 2,5-BHMF diol display T_{d50%} at temperatures between 262 and 311 °C (Table S3). As it can be observed, for most samples the thermal degradation occurs in a single step. For some samples, as those derived from 2,5-BHMF, a second step, that takes place at higher temperature, has been detected (the corresponding T_{max} has been added to Supplementary Table 3).

2.2. Synthesis of pyridine diols-based polyesters and comparison with their petroleum-based counterpart

After synthesizing a series of aliphatic-aromatic polyesters based on furan diols, following our recent work on the substitution of

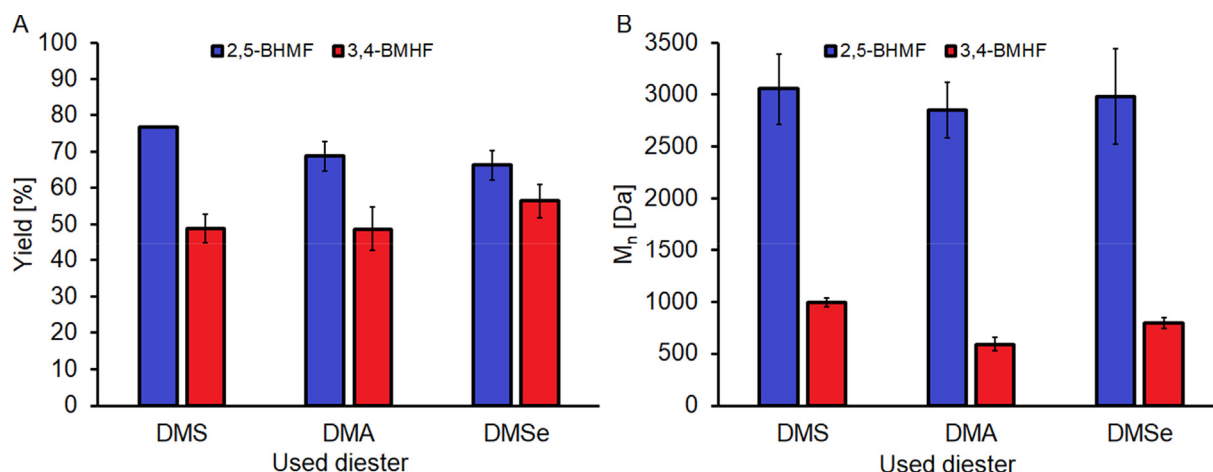


Fig. 1. Comparison of the two furan-based diols used in this study. A) Isolated yield and B) polymer's number average molecular weights (M_n). Blue bars = 2,5-BHMF, red bars = 3,4-BHMF. All reactions were conducted in duplicates. The figure shows the average of two experiments \pm the standard deviation. (For interpretation of the references to colour in this figure legend, the reader is referred to the web version of this article.)

terephthalic and isophthalic acids using lignin-derived pyridine-based diesters [17], the interest moved to the possibility of imparting rigidity to the polymer's chain using some pyridine-based diols. Amongst them we selected the commercially available 2,6-bis(hydroxymethyl)pyridine (2,6-BHMP) that despite not being currently produced from biomass could be easily derived from the reduction of dipicolinic acid (DPA). DPA can constitute up to 10% wt (dry) of some bacterial spores [23] and has also been successfully produced from glucose fermentation via engineered *E. coli* [24]. The reduction of DPA (or its methyl diester) to 2,6-BHMP has been reported in numerous previous studies, typically involving the use of common reducing agents such as sodium borohydride [25] or lithium aluminium hydride [26]. We compared the 2,6-BHMP-based polyesters with their petroleum-based counterpart that were synthesized using 1,3-bis(hydroxymethyl)benzene (1,3-BHMB) as the aromatic diol.

Fig. 3A shows that while the yields obtained when the two diols are reacted with the C_4 DMS are quite similar (91% for 2,6-BHMP vs 82% for 1,3-BHMB), the ones for the reactions conducted using DMA and DMSe deviate for these two aromatic diols. In fact, while the yields obtained using 1,3-BHMB as the diol progressively decrease with the increase of the ester's chain length (DMS to DMA to DMSe), the ones obtained using 2,6-BHMP drop to 56% for the reaction with DMA but raise again up to 83% when the synthesis is conducted with the C_{10} diester DMSe (see Supplementary Table 4 for the complete set of

polymer's isolated yields data).

From Fig. 3B it is possible to notice that while for the 1,3-BHMB-based polymers the M_n decreased with the increase of the diester's carbon chain length (following the yields trend plotted in Fig. 3A), in the case of the 2,6-BHMP-based polymers the M_n increases with the increase of the diester's chain length (from 1500 Da for DMS, to 3100 Da for DMA to 4100 Da for DMSe). See Supplementary Table 5 for the complete set of GPC data.

The DSC thermal profiles of the 2,6-BHMP and 1,3-BHMB adipate polyesters are very similar (Fig. 4A), showing a decreasing T_g (from 4 °C to -26 °C for 2,6-BHMP-based polymers and from -4 °C to -52 °C for the 1,3-BHMB-based polymers) with the increasing of the diester's aliphatic carbon chain length from C_4 (DMS) to C_{10} (DMSe). The T_m follows a similar trend, decreasing from 122 °C to 72 °C for the 2,6-BHMP and from 120 °C to 15 °C for the 1,3-BHMB-based polymers, respectively (see Supplementary Table 2 for the complete set of DSC data).

From the TGA thermograms (Fig. 4B) it is evident how the 1,3-BHMB polymers ($T_{d50\%}$ = 388–406 °C) are more stable than the 2,6-BHMP-based ones ($T_{d50\%}$ = 339–369 °C) (see Supplementary Table 3 for the complete set of TGA data). This difference in the polymer's degradation temperature and the higher amount of matter left at the end of the analysis (residual mass at 625 °C: 5–13% for 1,3-BHMB-based polymers and 15–21% for 2,6-BHMP-based polymers) are in line with previous data reported using various pyridine diester monomers (and

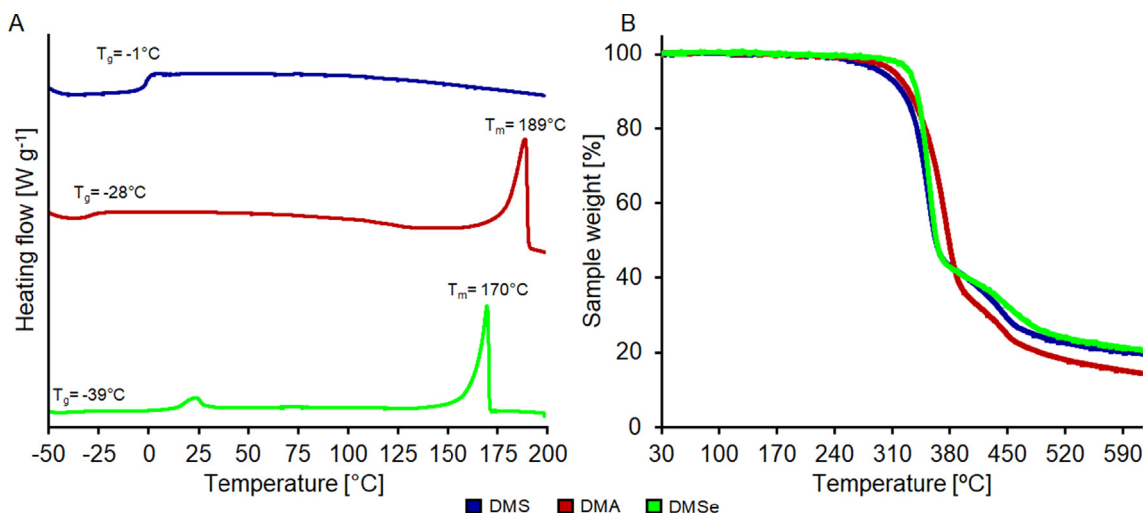


Fig. 2. Thermal analysis of the 3,4-BHMF-based polymers. (A) DSC analysis and (B) TGA analysis. T_g = glass transition temperature, T_m = melting temperature.

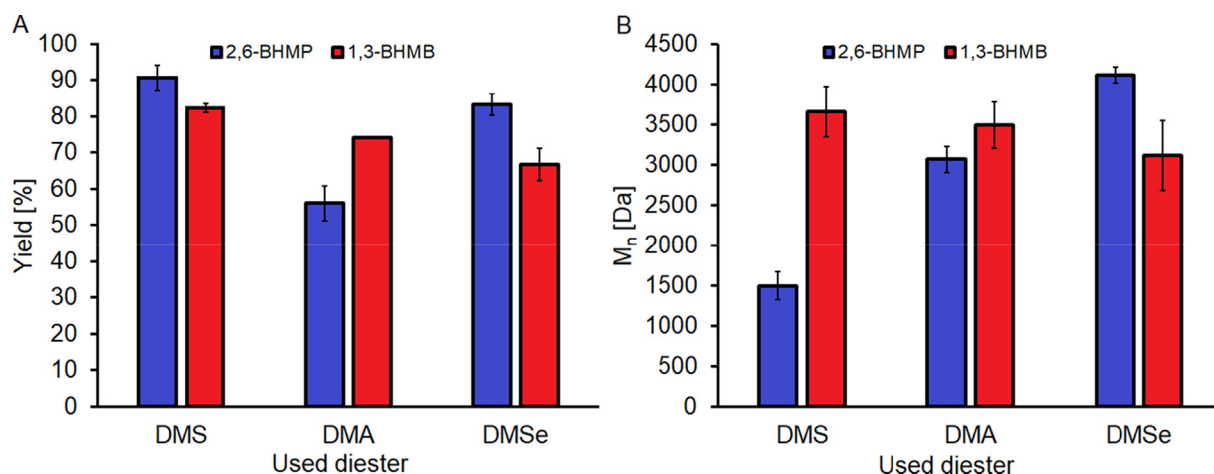


Fig. 3. Comparison of the pyridine-based diol with its benzene-based counterpart. (A) Isolated yield and (B) polymer's number average molecular weights (M_n). Blue bars = 2,6-BHMP, red bars = 1,3-BHMB. All reactions were conducted in duplicates. The figure shows the average of two experiments \pm the standard deviation. (For interpretation of the references to colour in this figure legend, the reader is referred to the web version of this article.)

their comparison with the petroleum-based alternatives) [17].

2.3. Comparison of various benzene-based diols and evaluation of the material's thermal properties.

After the successful synthesis of furan diols and pyridine diols-based polymers, the work was continued with the evaluation of additional petroleum-based diols such as 1,4-Bis(2-hydroxymethyl)benzene (1,4-BHMB) and 1,4-Bis(2-hydroxyethyl)benzene (1,4-BHEB). The selection of these diols was performed to establish if our enzymatic polycondensation method leads to products having major differences when using the 1,4- instead of the 1,3-regioisomer and the effect of an additional carbon (diol's hydroxyethyl derivative) on the thermal properties of the obtained polyester.

Comparing the reactions between the 1,4-BHMB and 1,4-BHEB diols and the various aliphatic diesters, it was observed that there were no significant differences in terms of isolated yields (Fig. 5A), with all reactions yielding between 67% and 86% and therefore similar to the yields isolated for the pyridine diol-based polymers. It was observed for both benzene diol polyesters that the M_n increases with the longer aliphatic carbon chains of the diester (Fig. 5B), for example poly(1,4-BHMB sebacate) resulted in the highest observed molecular masses

($M_n = 6700$ Da, $M_w = 31,100$ Da, $\bar{D} = 4.60$).

The main differences between the 1,4-BHMB- and 1,4-BHEB-based polymers are evident from the thermal analysis. Fig. 6A shows an increase of the crystallinity with the increase of the aliphatic ester's carbon chain length for the 1,4-BHMB-based polymers, with results that are in line with what observed using the furan-based diols. The DSC analysis of the 1,4-BHEB polymers, Fig. 6B, shows instead that adding one extra carbon into the hydroxyalkyl moiety of the aromatic diol results in all synthesized polymers to having more crystalline character.

As expected, the T_m of the polymers decreases with the increase of the aliphatic carbon chain length. From TGA analysis (Fig. 6C and D) it is possible to observe that the $T_{d50\%}$ of the 1,4-BHMB- and 1,4-BHEB-based polymers is rather similar, with $T_{d50\%}$ of $383 < T < 394$ °C and $390 < T < 415$ °C respectively (see Supplementary Table 3 for the complete set of TGA data).

2.4. Use of various aliphatic diesters as monomers for the enzymatic polycondensation reaction.

As an additional variation in the experimental conditions, we carried out the synthesis of poly(1,4-BHEB adipate) using various adipic acid diesters having MeOH (dimethyl adipate, DMA), EtOH (diethyl

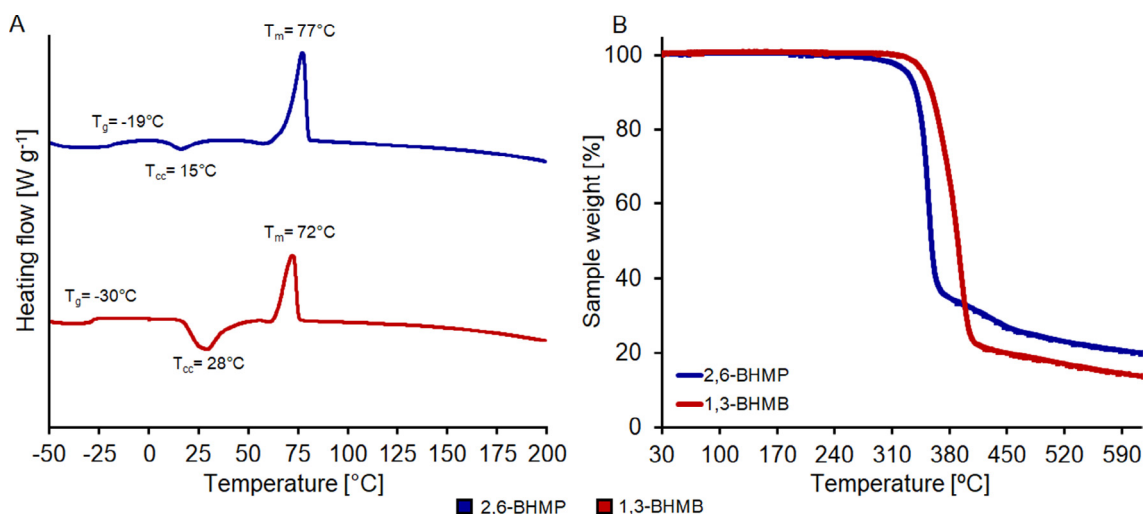


Fig. 4. Thermal analysis of 2,6-BHMP- and 1,3-BHMB-based polymers when combined with DMA as the diester. (A) DSC analysis and (B) TGA analysis of the polymers synthesized using dimethyl adipate (DMA) as the aliphatic diester. T_g = glass transition temperature, T_{cc} = cold crystallization temperature, T_m = melting temperature.

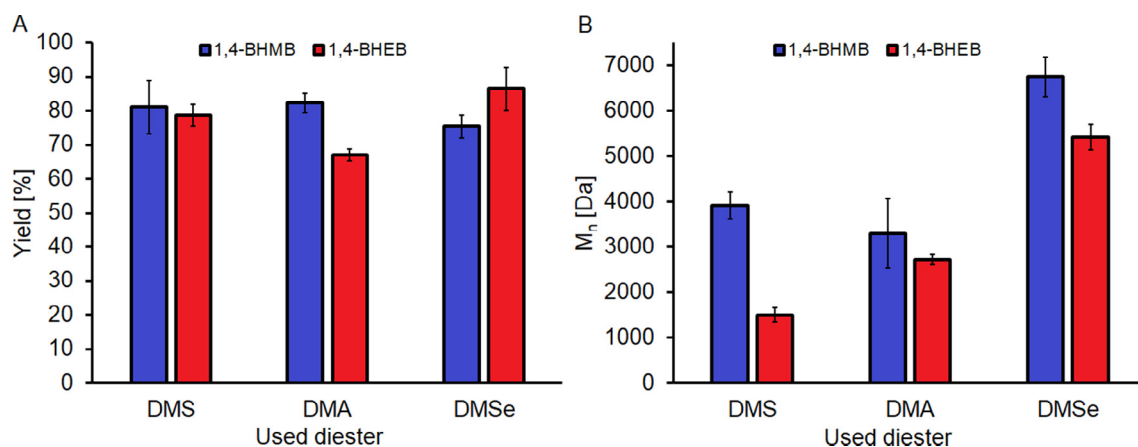


Fig. 5. Comparison of 1,4-BHMB with its hydroxyethyl counterpart, 1,4-BHEB. (A) Isolated yield and (B) polymer's number average molecular weights (M_n). Blue bars = 1,4-BHMB, red bars = 1,4-BHEB. All reactions were conducted in duplicates. The figure shows the average of two experiments \pm the standard deviation. (For interpretation of the references to colour in this figure legend, the reader is referred to the web version of this article.)

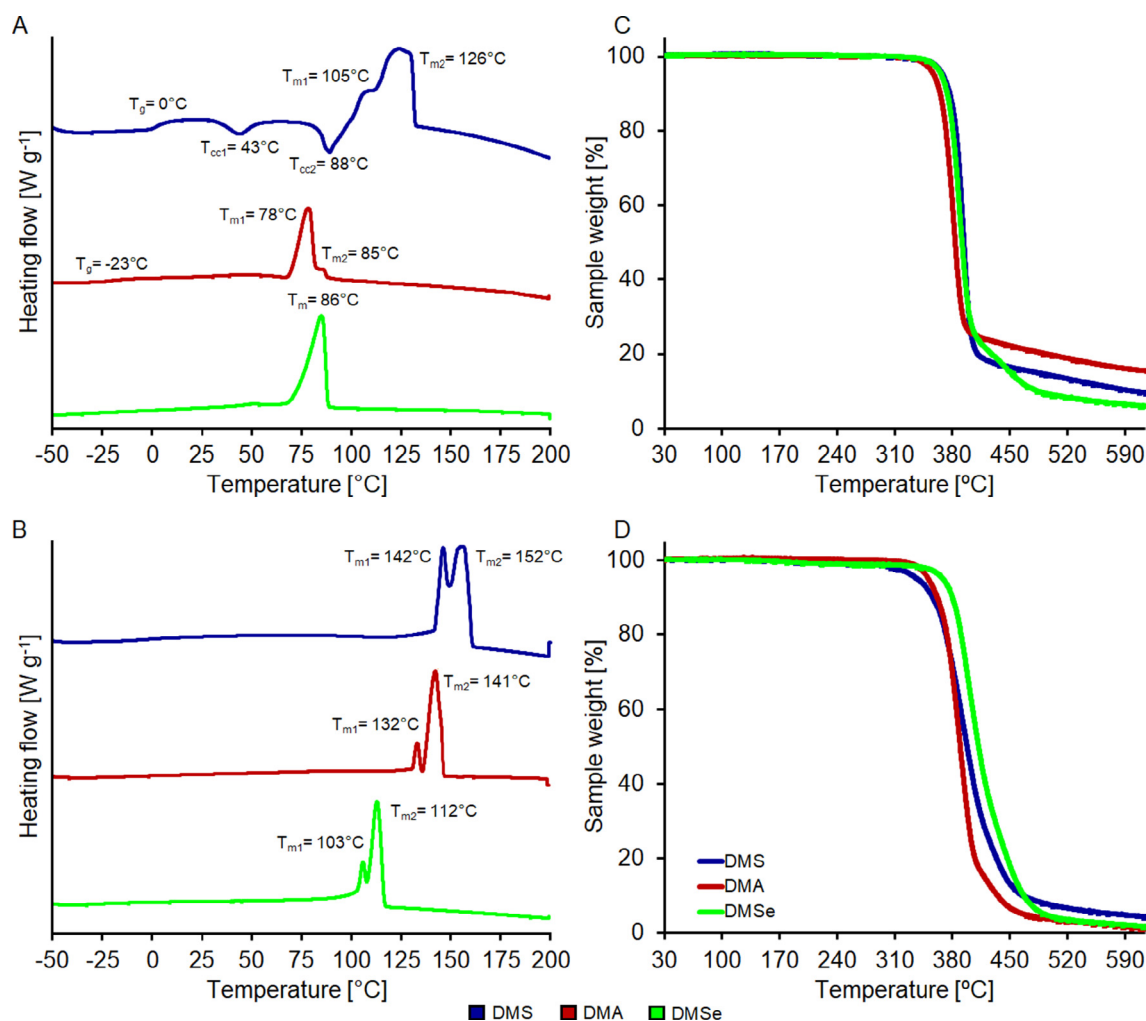


Fig. 6. Thermal analysis of 1,4-BHMB- (A and C) and 1,4-BHEB-based polymers (B and D). (A and B) DSC analysis and (C and D) TGA analysis of the polymers synthesized using dimethyl succinate (DMS, blue line), dimethyl adipate (DMA, red line) and dimethyl sebacate (DMSe, green line) as the aliphatic diester. T_g = glass transition temperature, T_{cc} = cold crystallization temperature, T_m = melting temperature. (For interpretation of the references to colour in this figure legend, the reader is referred to the web version of this article.)

adipate, DEA) or n-BuOH (DBA, dibutyl adipate) as leaving group and condensate. It is in fact known that, for enzymatic solventless polymerizations, a more volatile condensate (MeOH vs n-BuOH) leads to a better elongation of the polymer's chain [27,28]. In our case, changing

the diester's leaving group did not result in significant differences in terms of recovered yield (67–72%) nor in the obtained M_n (2600–3200 Da). The working hypothesis is that, in a solvent-based dilute system (monomer's concentration = 0.2 M) like the one used in

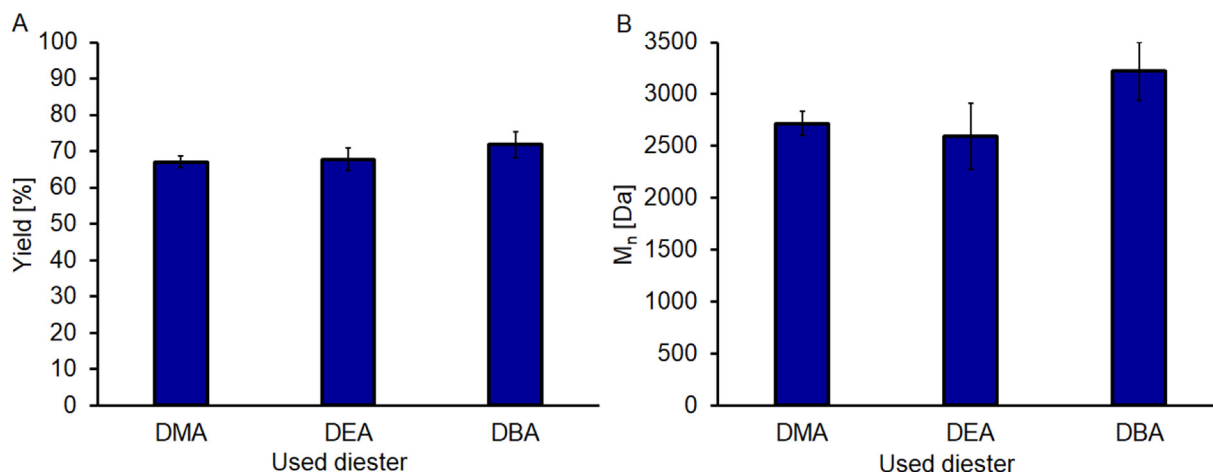


Fig. 7. Synthesis of poly(1,4-BHEB adipate) using various esters. (A) Isolated yield and (B) polymer's number average molecular weights (M_n). DMA = dimethyl adipate, DEA = diethyl adipate and DBA = dibutyl adipate. All reactions were conducted in duplicates. The figure shows the average of two experiments \pm the standard deviation.

this work, the released by-product stays in the reaction system for a longer time if compared with the solventless system (both systems being under vacuum), with the more polar MeOH causing a mayor inhibition of the biocatalyst if compared with the less polar n-BuOH. This hypothesis fits well with the observations that more polar solvents cause a mayor inhibition and therefore lead to lower yields and conversion rates when a CalB-catalyzed esterification is carried out [29] (see Fig. 7).

2.5. Polymer analysis and characterization

To complete the above reported data, ^1H NMR, FT-IR spectroscopy, MALDI and XRD characterization of the synthesized aromatic diols-based polyesters were also performed. ^1H NMR analysis confirmed the expected structure for all the studied polyesters (please see Supplementary Figs. 1–6 for the spectra of selected samples with the peak assignments).

FT-IR analysis of the synthesized materials was carried out to attempt a discrimination of the various polymers based on their near infrared spectra. In fact, in plastic recycling facilities this is the election technique for plastic separation [30]. Not surprisingly, in this case it is not easily possible to differentiate between the various aromatic diols because they all present some characteristic bands corresponding to: $2924\text{--}2936\text{ cm}^{-1}$ (two bands) symmetric and asymmetric stretching vibrations of the $-\text{CH}_2$ groups; $1728\text{--}1732\text{ cm}^{-1}$ (marked band) is due to the $\text{C}=\text{O}$ stretching vibrations; $1563\text{--}1595\text{ cm}^{-1}$ (one or two bands) corresponds to the $\text{C}=\text{C}$ stretching vibrations of the ring. Below the peaks at $\sim 1550\text{ cm}^{-1}$ fall all remaining bands from the aliphatic component and the bands corresponding to various group's vibrations (see Supplementary Figs. 7–12 for selected FT-IR spectra of the synthesized polymers).

MALDI analysis also confirm the molecular weights distributions observed with the GPC analysis and highlights the classical end groups (ester-diol, ester-ester, diol-diol and cyclic) expected for the class of polymers synthesized in the present work (see Supplementary Figs. 13–20 for selected MALDI spectra of the synthesized polymers). If we observe more in detail the ^1H NMR spectra plotted in the ESI, we can observe that at around 4.5 ppm some small resonances appear. This could be due to the BHMF $-\text{OH}$ groups that, being very reactive, they can dehydrate together to form ethers groups and this can lead to the blockage of the chain growth.

2,5-BHMF based polyesters display very similar WAXD patterns to those previously published indicating the development of the same crystal structures, and the same trend of the crystallinity degree (X_c),

which increases with the increase of the number of methylene units along the carboxylic subunit. These results support the DSC data and further confirm that longer aliphatic backbones cause higher chain flexibility, thus favouring chain packing [18].

However, differently from the work of Jiang et al. [18], the values of X_c are much lower, being respectively equal to 14, 16 and 19% for pF_{25}S , pF_{25}A and pF_{25}Se , probably due to the different molecular weight distribution, i.e. higher dispersity index. The 3,4-BHMF based materials display an increased degree of crystallinity with respect to the 2,5-BHMF based counterparts, being for pF_{34}A and pF_{34}Se equal to 24% and 27%, respectively, although it should be taken in account the low polymerization degree of these materials ($\text{DP} \approx 3$). The increase of X_c due to the higher flexibility imparted by longer aliphatic chains is maintained also in the 1,4-BHMB based polyesters, as a degree of crystallinity equal to 13% and 16% has been calculated for succinic acid (pB_{14}S) and sebacic acid (pB_{14}Se) containing polymers, respectively. The pattern of pB_{14}S shows three main reflections located at 22.3° , 24.1° and 26° and less intense peaks at 27.5° , 29.4° and 31.9° . pB_{14}Se displays a different crystalline phase with three main diffraction peaks at 23.6° , 25.2° and 28.5° .

Last, but not least, an opposite trend of X_c has been observed for 2,6-BHMP based polyesters. Indeed, the succinic acid containing polymer (pP_{26}S) has a higher X_c (22%) as compared to the sebacic acid containing one (pP_{26}S , $X_c = 19\%$). This result, which seems to contradict those above reported, may be ascribed to the very different DP of the two materials (6 and 13, respectively) that prevents a direct comparison of the measured values. The diffraction patterns of the two polymers highlight the development of a different crystalline phase, with pP_{26}S showing three main reflections, two intense and sharp at 20.5° and 28.3° and one less intense and broader at 24.3° . On the other hand, pP_{26}Se pattern is characterized by four main peaks, which are located at 20.17° , 24.7° , 27.6° and 30.9° .

3. Conclusions

The present work sheds light on the possibility of synthesizing bio-based polyesters from several furan and pyridine diols such as 2,5-bis(hydroxymethyl)furan (2,5-BHMF), 3,4-bis(hydroxymethyl)furan (3,4-BHMF) and 2,6-bis(hydroxymethyl)pyridine via enzymatic catalysis using a diphenyl ether-based reaction system. All polycondensation reactions were successful and gave isolated yields $> 65\%$ except the 3,4-BHMF polymers that yielded only $\sim 50\%$. The 2,5-BHMF polyesters are reported to have M_n of $\sim 3000\text{ Da}$ while the 2,6-BHMP-based ones have M_n s between 1500 Da and 4000 Da , depending on the aliphatic

diester used. The thermal behavior of the obtained polymers was also investigated and strict correlations between the used diol and the diester's aliphatic carbon chain length were highlighted. All polymers were compared with some benzene-based aromatic diesters, whose properties were also fully characterized. Additional ^1H NMR, FT-IR spectroscopy, MALDI and XRD analyses fully confirmed the structures and properties of the obtained materials.

4. Materials and methods

4.1. Chemicals and enzymes

1,4-Bis(2-hydroxyethyl)benzene (> 98%, 1,4-BHEB) was purchased from TCI. 2,5-bis(hydroxymethyl)furan (2,5-BHMF) was purchased from Apollo Scientific. 1,8-octanediol (ODO) was purchased from Acros Organics. 1,3-Bis(2-hydroxymethyl)benzene (98%, 1,3-BHMB), 1,4-Bis(2-hydroxymethyl)benzene (99%, 1,4-BHMB), 2,6-Bis(hydroxymethyl)pyridine (98%, 2,6-BHMP), 3,4-bis(hydroxymethyl)furan (98%, 3,4-BHMF), dimethyl succinate (DMS), dimethyl adipate (DMA), dimethyl sebacate (DMSe), diphenyl ether (DPE), and all other chemicals and solvents were purchased from Sigma-Aldrich and used as received if not otherwise specified.

Candida antarctica lipase B (CaLB) immobilized onto acrylic resin (iCaLB) was purchased from Sigma-Aldrich (product code L4777). The enzyme was vacuum dried for 48 h and stored in a desiccator before use.

4.2. Enzymatic polycondensation reactions in DPE

Synthesis were performed with a previously reported method [17]. Briefly, 8×10^{-4} mol of diester (0.2 M) and 8×10^{-4} mol of aromatic diol (0.2 M) (diester:diol ratio = 1:1) were added together with 4 mL of DPE in a 25-mL round bottom flask. The mixture was then stirred at 85 °C until complete dissolution of the monomers. In total, 10% w w $^{-1}$ (calculated on the total amount of the monomers) of iCaLB was then added and the reaction was run for 6 h at 1000 mbar. A vacuum of 20 mbar was subsequently applied for an additional 90 h while maintaining the reaction temperature at 85 °C. Warm chloroform was added to the mixture in order to fully solubilize the reaction product. The biocatalyst was then removed via a single filtration step and the solvent was distilled off using a rotary evaporator. The polymer was subsequently precipitated in ice-cold methanol and washed three times to remove all residual DPE. The reactions led to yellow to white powdery polymerization products. All reactions were performed in duplicate to ensure the reproducibility of the method.

4.3. Nuclear magnetic resonance (NMR) spectroscopy

^1H NMR spectroscopy analyses were performed on a JEOL JNM-ECS400A spectrometer at a frequency of 400 MHz for ^1H . CDCl_3 was used as NMR solvent for all polymers (see [Supplementary Figs. 1–6](#) for the fully assigned ^1H NMR spectra of some selected polymers).

4.4. Gel permeation chromatography (GPC)

GPC analysis were performed using a previously established method [17]. Samples were dissolved in CHCl_3 at a concentration of ~ 2 mg mL $^{-1}$ and filtered through cotton prior to addition in a HPLC vial. Gel permeation chromatography was carried out at 30 °C on an Agilent Technologies HPLC System (Agilent Technologies 1260 Infinity) connected to a 17,369 6.0 mm ID \times 40 mm L HHR-H, 5 μm Guard column and a 18,055 7.8 mm ID \times 300 mm L GMHHR-N, 5 μm TSKgel liquid chromatography column (Tosoh Bioscience, Tessenderlo, Belgium) using 1 mL min $^{-1}$ CHCl_3 as mobile phase. An Agilent Technologies G1362A refractive index detector was employed for detection. The molecular weights of the polymers were calculated using linear

polystyrene calibration standards. See [Supplementary Figs. 21–28](#) for the GPC chromatograms of selected samples.

4.5. Matrix assisted laser desorption ionization (MALDI)

MALDI-TOF MS analysis were carried by using a Bruker Solarix-XR FTICR mass spectrometer and the relative software package for the acquisition and the processing of the data. An acceleration voltage of 25 kV, using DCTB as matrix and KTFA as ionization agent were used. Ten microliters of sample were mixed with 10 μL of matrix solution (40 mg mL $^{-1}$ DCTB in CHCl_3) and 3 μL of KTFA (5 mg mL $^{-1}$). In total, 0.3 μL of the mixture were applied on the plate and the measurement was conducted in positive mode with the detector set in reflector mode.

4.6. Differential scanning calorimetry (DSC)

DSC analysis were performed using a TA Instruments Q2000 DSC under an inert gas atmosphere (N_2). The used heating and cooling rates were set to 5 °C over the -60 to 200 °C temperature range. Weighted sample masses in the range 5–10 mg were used. T_g , T_c and T_m values were reported from the second heating scan. The melting points of the starting compounds were also determined and are reported in [Supplementary Table 1](#). The complete set of the polymer's DSC data is reported in [Supplementary Table 2](#).

4.7. Thermogravimetric analysis (TGA)

TGA analysis were performed using a PL Thermal Sciences STA 625 thermal analyzer. ~ 10 mg of accurately weighed sample in an aluminum pan was placed into the furnace with a N_2 flow of 100 mL min $^{-1}$ and heated from 30 °C to 625 °C at a heating rate of 10 °C min $^{-1}$. From the TGA profiles the temperatures at 5, 10 and 50% mass loss (T_{d5} , T_{d10} and T_{d50} , respectively) were subsequently determined. All TGA data are summarized in [Supplementary Table 1](#) and selected samples are plotted as [Supplementary Figs. 29–38](#).

4.8. Fourier transformation infrared spectroscopy

FT-IR analysis were performed using a PerkinElmer 400 spectrometer using the attenuation total reflectance setting. The same pressure was applied on the outer surface of all analyzed samples. 32 scans were recorded for each sample using a 4 cm $^{-1}$ resolution. All spectra were processed using the automated baseline correction and the data auto-tune functions (see [Supplementary Figs. 7–12](#) for the FT-IR of selected samples).

4.9. X-ray diffractometry

The samples were measured between 5 and 52° 2 θ on a Panalytical Empyrean X-ray diffractometer equipped with Co Ka (1.790307 Å) radiation. They were mounted on a zero-background offset Si holder and a beam knife used to reduce the air scatter at low angle. See [Supplementary Figs. 39–46](#) for the XRD analysis of selected samples. The degree of crystallinity (X_c) was calculated from the XRD profiles as the ratio between the crystalline diffraction area (A_c) and the total diffraction area (A_t), according to:

$$X_c = (A_c/A_t) \times 100$$

The crystalline diffraction area was obtained by subtraction of the amorphous halo, modelled as bell shaped peak baseline, from the total area of the diffraction profile.

Declaration of Competing Interest

The authors declare that they have no known competing financial

interests or personal relationships that could have appeared to influence the work reported in this paper.

Acknowledgements

Alessandro Pellis thanks the FWF Erwin Schrödinger fellowship (grant agreement J 4014-N34) for financial support. Thomas J. Farmer thanks the Biotechnology and Biological Sciences Research Council (BBSRC, grant BB/N023595/1) for funding their involvement in this research. The authors thank Biome bioplastics Ltd. for financial support. All authors would like to thank Dr. David Walker from the University of Warwick for recording the XRD spectra.

Author contributions

A.P. performed the enzymatic polymer synthesis and the polymer characterizations, planned the experiments and wrote the manuscript. S.W. performed the GPC analysis of the polymers. M. G. performed the XRD data analysis, wrote the relative discussion and analyzed the DTG curves. G.M.G. and T.J.F. supervised the work. G.M.G., M.G. and T.J.F. contributed with discussions and manuscript revisions. All authors corrected the manuscript and discussed the data prior to submission.

Data availability

All data used in the preparation of this manuscript is contained within this document, included in the electronic [supplementary information](#) file or available from DOI: [10.15124/73d14ed1-52b1-4a0f-bf32-0b4766e81bf8](https://doi.org/10.15124/73d14ed1-52b1-4a0f-bf32-0b4766e81bf8).

Appendix A. Supplementary material

Supplementary data to this article can be found online at <https://doi.org/10.1016/j.eurpolymj.2020.109680>.

References

- https://europa.eu/rapid/press-release_IP-18-5_en.htm (Link accessed on 24.10.2019).
- G.Z. Papageorgiou, V. Tsanakis, D.N. Bikiaris, Synthesis of poly(ethylene furandicarboxylate) polyester using monomers derived from renewable resources: thermal behavior comparison with PET and PEN, *Phys. Chem. Chem. Phys.* **16** (2014) 7946–7958.
- A. Pellis, E. Herrero Acero, V. Ferrario, D. Ribitsch, G.M. Guebitz, L. Gardossi, The closure of the cycle: enzymatic synthesis and functionalization of bio-based polyesters, *Trends Biotechnol.* **34** (2016) 316–328.
- J.K. Ogunjobi, T.J. Farmer, C.R. McElroy, S.W. Breeden, D.J. Macquarrie, D. Thornthwaite, J.H. Clark, Synthesis of biobased diethyl terephthalate via diels-alder addition of ethylene to 2,5-furandicarboxylic acid diethyl ester: an alternative route to 100% biobased poly(ethylene terephthalate), *ACS Sustain. Chem. Eng.* **7** (2019) 8183–8194.
- G.Z. Papageorgiou, V. Tsanakis, D.G. Papageorgiou, K. Chrissafis, S. Exarhopoulos, D.N. Bikiaris, Furan-based polyesters from renewable resources: Crystallization and thermal degradation behavior of poly(hexamethylene 2,5-furandicarboxylate), *Eur. Polym. J.* **67** (2015) 383–396.
- A. Gandini, A.J.D. Silvestre, C. Pascoal Neto, A.F. Sousa, M. Gomes, The furan counterpart of poly(ethylene terephthalate): An alternative material based on renewable resources, *J. Polym. Sci. Part A Polym. Chem.* **47** (2009) 295–298.
- Y. Jiang, A.J.J. Woortman, G.O.R. Alberda van Ekenstein, K. Loos, A biocatalytic approach towards sustainable furanic-aliphatic polyesters, *Polym. Chem.* **6** (2015) 5198–5211.
- Y. Jiang, D. Maniar, A.J.J. Woortman, K. Loos, Enzymatic synthesis of 2,5-furandicarboxylic acid-based semi-aromatic polyamides: enzymatic polymerization kinetics, effect of diamine chain length and thermal properties, *RSC Adv.* **6** (2016) 67941–67953.
- J. Zhu, J. Cai, W. Xie, P.-H. Chen, M. Gazzano, M. Scandola, R.A. Gross, Poly(butylene 2,5-furan dicarboxylate), a biobased alternative to PBT: synthesis, physical properties, and crystal structure, *Macromolecules* **46** (2013) 796–804.
- G. Guidotti, M. Gigli, M. Soccio, N. Lotti, M. Gazzano, V. Siracusa, A. Munari, Poly(butylene 2,5-thiophenedicarboxylate): an added value to the class of high gas barrier biopolyesters, *Polymers* **10** (2018) 167.
- M. Gigli, F. Quartinello, M. Soccio, A. Pellis, N. Lotti, G.M. Guebitz, S. Licoccia, A. Munari, Enzymatic hydrolysis of poly(1,4-butylene 2,5-thiophenedicarboxylate) (PBTf) and poly(1,4-butylene 2,5-furandicarboxylate) (PBF) films: a comparison of mechanisms, *Environ. Int.* **130** (2019) 104852(1–7).
- G. Guidotti, M. Gigli, M. Soccio, N. Lotti, M. Gazzano, V. Siracusa, A. Munari, Ordered structures of poly(butylene 2,5-thiophenedicarboxylate) and their impact on material functional properties, *Eur. Polym. J.* **106** (2018) 284–290.
- A.F. Sousa, C. Vilela, A.C. Fonseca, M. Matos, C.S.R. Freire, J.-J.M. Gruter, J.F.J. Coelho, A.J.D. Silvestre, Biobased polyesters and other polymers from 2,5-furandicarboxylic acid: a tribute to furan excellency, *Polym. Chem.* **6** (2015) 5961–5983.
- C. Gamerith, M. Vastano, S.M. Ghorbanpour, S. Zitzenbacher, D. Ribitsch, M.T. Zumstein, M. Sander, E. Herrero Acero, A. Pellis, G.M. Guebitz, Enzymatic degradation of aromatic and aliphatic polyesters by *P. pastoris* expressed cutinase 1 from *Thermobifida cellulolytica*, *Front. Microbiol.* **8** (2017) 938.
- R. Wei, W. Zimmermann, Microbial enzymes for the recycling of recalcitrant petroleum-based plastics: how far are we? *Microb. Biotechnol.* **10** (2017) 1308–1322.
- S. Weinberger, J. Canadell, F. Quartinello, B. Yeniad, A. Arias, A. Pellis, G.M. Guebitz, Enzymatic degradation of poly(ethylene 2,5-furanoate) powders and amorphous films, *Catalysts* **7** (2017) 318, <https://doi.org/10.3390/catal7110318>.
- A. Pellis, J.W. Comerford, S. Weinberger, G.M. Guebitz, J.H. Clark, T.J. Farmer, Enzymatic synthesis of lignin derivable pyridine based polyesters for the substitution of petroleum derived plastics, *Nat. Commun.* **10** (2019) 1762, <https://doi.org/10.1038/s41467-019-09817-3>.
- Y. Jiang, A.J.J. Woortman, G.O.R. Alberda van Ekenstein, D.M. Petrović, K. Loos, Enzymatic synthesis of biobased polyesters using 2,5-Bis(hydroxymethyl)furan as the building block, *Biomacromolecules* **15** (2014) 2482–2493.
- D. Maniar, Y. Jiang, A.J.J. Woortman, J. van Dijken, K. Loos, Furan-based copolyesters from renewable resources: enzymatic synthesis and properties, *ChemSusChem* **12** (2019) 990–999.
- C. Lavilla, A. Martínez de Ilarduya, A. Alla, M.G. García-Martín, J.A. Galbis, S. Muñoz-Guerra, Bio-based aromatic polyesters from a novel bicyclic diol derived from d-mannitol, *Macromolecules* **45** (2012) 8257–8266.
- J. Wu, P. Eduard, S. Thiyagarajan, B.A.J. Noordover, D.S. van Es, C.E. Koning, Semi-aromatic polyesters based on a carbohydrate-derived rigid diol for engineering plastics, *ChemSusChem* **8** (2015) 67–72.
- L. Gustini, C. Lavilla, A. Martínez de Ilarduya, S. Muñoz-Guerra, C.E. Koning, Isohexide and sorbitol-derived, enzymatically synthesized renewable polyesters with enhanced Tg, *Biomacromolecules* **17** (2016) 3404–3416.
- T.A. Slieman, W.L. Nicholson, Role of dipicolinic acid in survival of bacillus subtilis spores exposed to artificial and solar UV radiation, *Appl. Environ. Microbiol.* **67** (2001) 1274–1279.
- M.K. McClintock, G.W. Fahnhorst, T.R. Hoyer, K. Zhang, Engineering the production of dipicolinic acid in *E. coli*, *Metab. Eng.* **48** (2018) 208–217.
- A.J. Wessel, J.W. Schultz, F. Tang, H. Duana, L.M. Mirica, Improved synthesis of symmetrically & asymmetrically N-substituted pyridinophane derivatives, *Org. Biomol. Chem.* **15** (2017) 9923–9931.
- Z. He, P.J. Chaimungkalanont, D.C. Craig, S.B. Colbran, Copper(II) complexes of 6-hydroxymethyl-substituted tris(2-pyridylmethyl)amine ligands, *J. Chem. Soc., Dalton Trans.* (2000) 1419–1429.
- A. Pellis, P.A. Hanson, J.W. Comerford, J.H. Clark, T.J. Farmer, Enzymatic synthesis of unsaturated polyesters: functionalization and reversibility of the aza-Michael addition of pendants, *Polym. Chem.* **10** (2019) 843–851, <https://doi.org/10.1039/C8PY01655K>.
- A. Pellis, J.W. Comerford, A.J. Maneffa, M.H. Sipponen, J.H. Clark, T.J. Farmer, Elucidating enzymatic polymerisations: Chain-length selectivity of Candida antarctica lipase B towards various aliphatic diols and dicarboxylic acid diesters, *Eur. Polym. J.* **106** (2018) 79–84, <https://doi.org/10.1016/j.eurpolymj.2018.07.009>.
- A. Iemhoff, J. Sherwood, C.R. McElroy, A.J. Hunt, Towards sustainable kinetic resolution, a combination of bio-catalysis, flow chemistry and bio-based solvents, *Green Chem.* **20** (2018) 136–140, <https://doi.org/10.1039/C7GC03177G>.
- Y. Zheng, J. Bai, J. Xu, X. Li, Y.A. Zhang, A discrimination model in waste plastics sorting using NIR hyperspectral imaging system, *Waste Manag.* **72** (2018) 87–98, <https://doi.org/10.1016/j.wasman.2017.10.015>.